STEEL GRAVITY CONNECTIONS SUBJECTED TO LARGE ROTATIONS AND AXIAL LOADS

Jonathan M. Weigand
National Institute of Standards and Technology, Gaithersburg, MD 20899, USA
jonathan.weigand@nist.gov

Jeffrey W. Berman
University of Washington, Seattle, WA 98195, USA
jwberman@uw.edu

ABSTRACT

Steel gravity framing systems (SGFSs) rely on connections for system robustness when a column suffers damage that compromises its ability to carry gravity loads. Redistribution of gravity loads through the development of a sustained tensile configuration resulting from large vertical deflections is a key behavior in achieving robustness. Development of such an alternative load path depends on the ability of the gravity connections to remain intact after undergoing large rotation and axial extension demands. These demands are significantly larger than those considered for typical SGFS connection design. This paper presents the results of experiments on steel single-plate shear and bolted angle connections subjected to loading consistent with an interior column removal. The characteristic connection behaviors are described and the performance of multiple connection configurations are compared in terms of their peak resistances and deformation capacities.

INTRODUCTION

Steel gravity framing systems (SGFSs) are present in nearly every steel building constructed in the United States, yet they have been identified as potentially vulnerable to collapse (Foley et al., 2006; Sadek et al., 2008; Main and Sadek, 2012; Weigand, 2014). If the vertical load carrying capacity of a single column is diminished or lost, it is presently unclear if the gravity loads on the structure can be sustained. The notion of a design procedure for achieving structural robustness in SGFSs is in its infancy, and the current body of knowledge lacks experimental data on the behavior and performance of steel buildings subjected to unanticipated loads.

While it would be impractical and prohibitively expensive to directly design for unanticipated loading events (e.g., vehicular impact, blast, or accidental overload), history has shown that some inherent robustness is often present. Research on disproportionate collapse in steel framing has found that ductile connection detailing may improve system robustness under unanticipated loadings. In the event that a column in a SGFS loses the capacity to support its gravity loads, alternative load paths must develop in the horizontal framing members to support the gravity loads. These load paths develop from large vertical deflections that result in catenary action in the system, and that subject the connections to large rotation and axial extension demands.

The performance of steel gravity connections under seismic loading has been studied experimentally. However, experimental investigations involving the collapse behavior of SGFSs or its components are more limited. Astaneh-Asl et al. (2001a) investigated the collapse resistance of a two-bay gravity system under column removal and showed that an improvement in capacity could be achieved (Astaneh-Asl et al., 2001c) by adding post-tensioning cables. Thompson (2009) tested specimens each consisting of a column stub with symmetrically configured single-plate shear connections tied via short stiffened pinned-end beams to a vertical perimeter frame under an interior column pulldown scenario. Using connection sub-assemblages, Guravich and Dawe (2006) conducted an investigation of four gravity connection types typical to Canadian structural engineering practice to determine if shear connections could sustain significant tensile loads in combination with their design shear capacity. Oosterhof and Driver (2012) also investigated the strength and ductility of common shear connections using sub-assemblages, under combinations of moment, shear, and tension.

To evaluate the structural robustness of SGFSs, a multi-university collaborative experimental program was established to investigate the behavior of the state of current industry practice for gravity framing and work toward developing the next-generation of SGFSs. This program was a collaborative effort which involved contributions from the University of Washington (UW), Purdue University (PU), and the University of Illinois at Urbana-Champaign (UIUC). This paper summarizes experimental results from tests on SGFS connection subassemblies conducted at the UW to evaluate their response to loading consistent with an interior column losing its vertical load carrying capacity. A broad range of single-plate shear and bolted angle connection sub-assemblage tests were conducted to characterize connection response to combined loading, and to determine controlling failure mechanisms for various connection geometries.

CONNECTION CONFIGURATIONS

The steel single-plate shear and bolted angle connection sub-assemblages tested in this study were designed to resist the shear demands resulting from a series of prototypical steel gravity framing systems, with gravity loads modeled after the SAC[1] prototype building loads. The prototype systems encompassed a broad range of configurations typical of current industry design practice, and are described in more detail in Weigand et al. (2012). The connection configurations were selected from the prototype system designs and refined to provide a wide breadth of parameter variation.

[1]SAC Joint Venture between the Structural Engineers Association of California (SEAOC), the Applied Technology Council (ATC), and the Consortium of Universities for Research in Earthquake Engineering (CUREE)

The typical connection sub-assemblage specimen consisted of a 1524 mm (60.0 in) long W12×72 column stub and a 1220 mm (48.0 in) long W21×50 beam stub, connected via a single shear plate (Fig. 1), bolted web angles, or top and seat angles; however, two specimens used W14×90 and W18×35 column and beam stub sections, respectively. The varied connection parameters for the single-plate shear connections included the number of bolts (n_b), bolt diameter (d_b), bolt grade, plate thickness (t_p), horizontal plate edge distance (L_{ehp}) relative to the minimum allowable plate edge distance (L_{emin}), hole type (standard (STD) or short-slotted (SSLT)), eccentricity with respect to the beam centerline, gap between the beam flange and the column flange, and the simulated system span. The varied connection parameters for the bolted angle specimens included the number of bolts on the angle legs bolted to the column flange (n_b), angle column-leg bolt diameter (Col. d_b), angle beam-leg bolt diameter (Bm. d_b), angle leg thickness (t_L), configuration, eccentricity with respect to the beam centerline, and gap between the beam flange and the column flange. The naming convention for the tested specimens consists of a prefix that describes the connection type (e.g., sps (Single-Plate Shear)), followed by the number of bolts (e.g., 3b), the hole type (e.g., STD), the bolt diameter fraction in inches (e.g., 34 corresponds to 3/4 in), plate thickness fraction in inches (e.g., 38 corresponds to 3/8 in), and additional descriptor (e.g., Edge) where applicable. A similar naming convention was used for the bolted angle connections using the bolt diameter fraction, angle thickness fraction, and additional descriptor, where applicable. Table 1 shows the parameter values for the single-plate shear specimens and Table 2 shows the values for the bolted angle specimens.

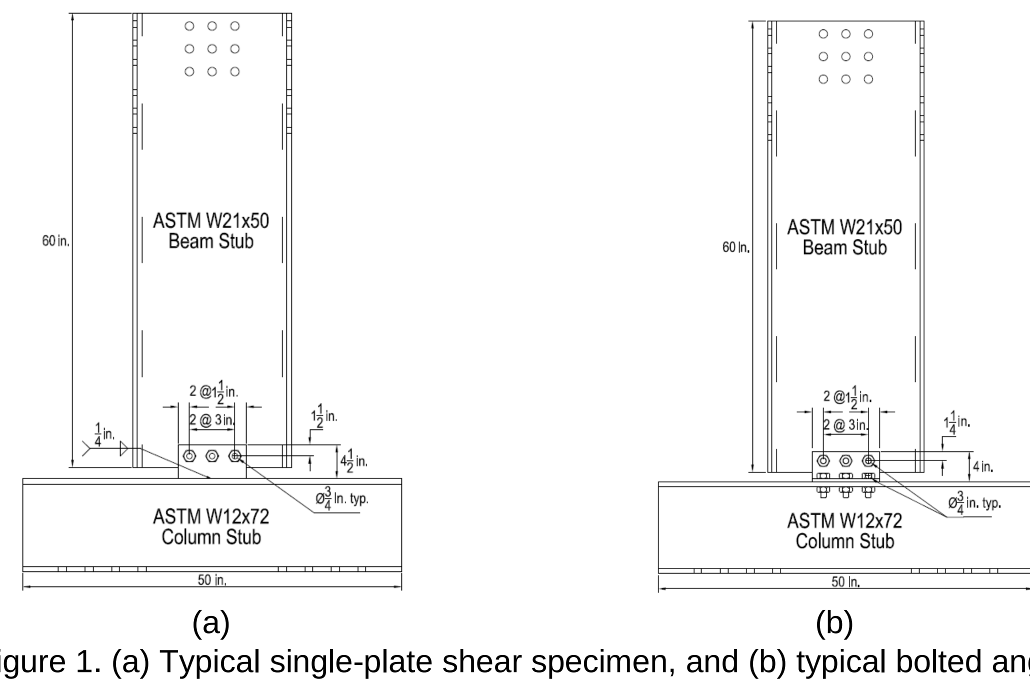

(a) (b)

Figure 1. (a) Typical single-plate shear specimen, and (b) typical bolted angle specimen (1 in = 25.4 mm). For both: dimensions vary, see Tables 1 and 2.

Name	Connection Properties	Test Results

<table>
<tr><th></th><th>Span (m)</th><th>n_b</th><th>d_b (mm)</th><th>t_p (mm)</th><th>Hole Type</th><th>L_{ehp}/L_{emin}</th><th>Δ (mm)</th><th>θ (rad)</th><th>δ (mm)</th><th>d_f (mm)</th><th>V_{max} (kN)</th><th>T_{max} (kN)</th><th>V_{max}/V_{Nom}</th><th>Failure Location</th></tr>
<tr><td>sps3b|STD|34|38|48L[1]</td><td>14.6</td><td>3</td><td>19.1</td><td>9.53</td><td>STD</td><td>1.5</td><td>1053</td><td>0.075</td><td>19.6</td><td>24.5</td><td>41.2</td><td>497</td><td>0.099</td><td>Bolt</td></tr>
<tr><td>sps4b|STD|34|38|48L[1]</td><td>14.6</td><td>4</td><td>19.1</td><td>9.53</td><td>STD</td><td>1.5</td><td>1159</td><td>0.082</td><td>23.8</td><td>32.7</td><td>55.1</td><td>647</td><td>0.093</td><td>Bolt</td></tr>
<tr><td>sps3b|STD|34|38|</td><td>9.1</td><td>3</td><td>19.1</td><td>9.53</td><td>STD</td><td>1.5</td><td>788</td><td>0.090</td><td>17.9</td><td>20.7</td><td>40.2</td><td>495</td><td>0.097</td><td>Bolt</td></tr>
<tr><td>sps3b|SSLT|34|38|</td><td>9.1</td><td>3</td><td>19.1</td><td>9.53</td><td>SSLT</td><td>1.5</td><td>890</td><td>0.092</td><td>22.7</td><td>24.5</td><td>44.1</td><td>474</td><td>0.106</td><td>Bolt</td></tr>
<tr><td>sps3b|SSLT|34|38|Edge</td><td>9.1</td><td>3</td><td>19.1</td><td>9.53</td><td>SSLT</td><td>1.0</td><td>809</td><td>0.087</td><td>18.8</td><td>22.4</td><td>32.3</td><td>384</td><td>0.067</td><td>Plate</td></tr>
<tr><td>sps4b|SSLT|34|38|</td><td>9.1</td><td>4</td><td>19.1</td><td>9.53</td><td>SSLT</td><td>1.5</td><td>863</td><td>0.093</td><td>21.4</td><td>24.2</td><td>49.6</td><td>544</td><td>0.083</td><td>Bolt</td></tr>
<tr><td>sps5b|SSLT|34|38|</td><td>9.1</td><td>5</td><td>19.1</td><td>9.53</td><td>SSLT</td><td>1.5</td><td>807</td><td>0.079</td><td>18.7</td><td>25.5</td><td>60.4</td><td>628</td><td>0.078</td><td>Bolt</td></tr>
<tr><td>sps3b|SSLT|34|38|A490</td><td>9.1</td><td>3</td><td>19.1</td><td>9.53</td><td>SSLT</td><td>1.5</td><td>943</td><td>0.099</td><td>25.5</td><td>28.7</td><td>52.4</td><td>527</td><td>0.119</td><td>Bolt</td></tr>
<tr><td>sps3b|SSLT|34|38|Offset[2]</td><td>9.1</td><td>3</td><td>19.1</td><td>9.53</td><td>SSLT</td><td>1.5</td><td>906</td><td>0.091</td><td>23.6</td><td>24.4</td><td>43.4</td><td>435</td><td>0.105</td><td>Bolt</td></tr>
<tr><td>sps4b|SSLT|78|38|</td><td>9.1</td><td>4</td><td>22.1</td><td>9.53</td><td>SSLT</td><td>1.3</td><td>795</td><td>0.081</td><td>18.2</td><td>22.7</td><td>48.7</td><td>503</td><td>0.081</td><td>Bolt</td></tr>
<tr><td>sps3b|SSLT|34|14|</td><td>9.1</td><td>3</td><td>19.1</td><td>6.35</td><td>SSLT</td><td>1.5</td><td>894</td><td>0.089</td><td>23.0</td><td>26.4</td><td>38.9</td><td>387</td><td>0.123</td><td>Plate</td></tr>
<tr><td>sps3b|SSLT|34|38|Gap[3]</td><td>9.1</td><td>3</td><td>19.1</td><td>9.53</td><td>SSLT</td><td>1.5</td><td>772</td><td>0.067</td><td>17.1</td><td>19.9</td><td>36.9</td><td>426</td><td>0.089</td><td>Bolt</td></tr>
<tr><td>sps3b|SSLT|34|14|Weak[4]</td><td>9.1</td><td>3</td><td>19.1</td><td>9.53</td><td>SSLT</td><td>1.5</td><td>972</td><td>0.110</td><td>27.1</td><td>32.6</td><td>38.5</td><td>388</td><td>0.121</td><td>Plate</td></tr>
</table>

Table 2. Bolted Angle Connection Test Specimens and Results

<table>
<tr><th rowspan="2">Name</th><th colspan="4">Connection Properties</th><th colspan="8">Test Results</th></tr>
<tr><th>n_b</th><th>Col d_b (mm)</th><th>Bm. d_b (mm)</th><th>t_L (mm)</th><th>Δ (mm)</th><th>θ (rad)</th><th>δ (mm)</th><th>d_f (mm)</th><th>V_{max} (kN)</th><th>T_{max} (kN)</th><th>V_{max}/V_{Nom}</th><th>Failure Location</th></tr>
<tr><td>ba3b|34|14|</td><td>3</td><td>19.1</td><td>19.1</td><td>6.35</td><td>1175</td><td>0.133</td><td>37.6</td><td>45.3</td><td>34.2</td><td>282</td><td>0.049</td><td>Angle</td></tr>
<tr><td>ba3b|34|12|</td><td>3</td><td>19.1</td><td>19.1</td><td>12.7</td><td>1168</td><td>0.132</td><td>37.2</td><td>41.6</td><td>61.1</td><td>543</td><td>0.067</td><td>Bolts</td></tr>
<tr><td>ba5b|34|14|</td><td>5</td><td>19.1</td><td>19.1</td><td>6.35</td><td>1033</td><td>0.117</td><td>29.3</td><td>46.7</td><td>46.4</td><td>373</td><td>0.041</td><td>Angle</td></tr>
<tr><td>ba5b|34|12|</td><td>5</td><td>19.1</td><td>19.1</td><td>12.7</td><td>1078</td><td>0.118</td><td>31.9</td><td>47.8</td><td>93.9</td><td>780</td><td>0.059</td><td>Bolts</td></tr>
<tr><td>ba3b|1|34|</td><td>3</td><td>25.4</td><td>25.4</td><td>19.1</td><td>1563</td><td>0.176</td><td>64.6</td><td>74.6</td><td>134.1</td><td>877</td><td>0.146</td><td>Beam Web</td></tr>
<tr><td>ba3b|34|14|Offset[1]</td><td>3</td><td>19.1</td><td>19.1</td><td>6.35</td><td>1074</td><td>0.122</td><td>31.7</td><td>41.1</td><td>33.0</td><td>258</td><td>0.047</td><td>Angle</td></tr>
<tr><td>ba3b|34|12|Offset[1]</td><td>3</td><td>19.1</td><td>19.1</td><td>12.7</td><td>1086</td><td>0.116</td><td>32.3</td><td>39.6</td><td>60.5</td><td>533</td><td>0.066</td><td>Bolts</td></tr>
<tr><td>ba3b|34|14|Gap[2]</td><td>3</td><td>19.1</td><td>19.1</td><td>6.35</td><td>1080</td><td>0.122</td><td>32.0</td><td>40.5</td><td>30.5</td><td>258</td><td>0.044</td><td>Angle</td></tr>
<tr><td>ba3b|34|12|Gap[2]</td><td>3</td><td>19.1</td><td>19.1</td><td>12.7</td><td>1150</td><td>0.122</td><td>36.1</td><td>41.2</td><td>65.2</td><td>553</td><td>0.071</td><td>Bolts</td></tr>
<tr><td>ba3b|34|14|TopSeat[3]</td><td>3</td><td>19.1</td><td>19.1</td><td>6.35</td><td>542</td><td>0.062</td><td>8.3</td><td>-</td><td>42.5</td><td>137</td><td>0.077</td><td>Angle</td></tr>
<tr><td>ba3b|34|12|TopSeat[3]</td><td>3</td><td>19.1</td><td>19.1</td><td>12.7</td><td>557</td><td>0.063</td><td>8.7</td><td>-</td><td>68.9</td><td>46</td><td>0.108</td><td>Bolts</td></tr>
<tr><td>ba3b|34|14|HConfig[4]</td><td>3</td><td>19.1</td><td>25.4</td><td>6.35</td><td>1328</td><td>0.15</td><td>47.6</td><td>52.9[8]</td><td>44.5</td><td>322</td><td>0.064</td><td>Angle</td></tr>
<tr><td>ba3b|34|12|HConfig[4]</td><td>3</td><td>19.1</td><td>25.4</td><td>12.7</td><td>1216</td><td>0.138</td><td>40.2</td><td>41.7[8]</td><td>57.8</td><td>475</td><td>0.063</td><td>Beam Web</td></tr>
<tr><td>ba3b|34|14|BlegWeld[5]</td><td>3</td><td>19.1</td><td>-</td><td>6.35</td><td>1067</td><td>0.121</td><td>31.2</td><td>-</td><td>27.2</td><td>240</td><td>0.039</td><td>Angle</td></tr>
<tr><td>ba3b|34|14|ClegWeld[6]</td><td>3</td><td>-</td><td>19.1</td><td>6.35</td><td>1125</td><td>0.127</td><td>34.6</td><td>34.1</td><td>15.8</td><td>130</td><td>0.023</td><td>Weld</td></tr>
<tr><td>ba3b|34|14|Weak[7]</td><td>3</td><td>19.1</td><td>19.1</td><td>6.35</td><td>1100</td><td>0.125</td><td>33.2</td><td>-</td><td>29.5</td><td>231</td><td>0.042</td><td>Angle</td></tr>
<tr><td>ba3b|34|14|Weak[7]</td><td>3</td><td>19.1</td><td>19.1</td><td>12.7</td><td>1373</td><td>0.155</td><td>50.6</td><td>-</td><td>79.6</td><td>591</td><td>0.087</td><td>Bolts</td></tr>
</table>

Note: All bolted angle specimens used a simulated span of 9.1 m (30 ft)

[1] Angles offset 76 mm (3.0 in) from beam centerline.

[2] Reduced gap of 6.4 mm (1/4 in) between beam flange and column flange.

[3] Top-and-seat angle configuration.

[4] Angles had three 19.1 mm (3/4 in) diameter bolts on column legs and two 25.4 mm (1 in) diameter bolts on beam legs.

[5] Angles bolted to column face and welded to beam web.

[6] Angles welded to column face and bolted to beam web.

[7] Weak-axis configuration that frames into column web.

[8] Value corresponds to fiber centered at beam leg bolt.

TEST SETUP AND LOADING

A self-reacting load frame (Fig. 2) was constructed in the UW Structural Research Laboratory. The reaction frame was capable of delivering combined shear, tension, and flexural loading to the gravity connection sub-assemblages. Three actuators were attached at their bases to the reaction frame and at their heads to a load beam. A single 245 kN (55 kip) actuator was mounted horizontally to the reaction column and attached to the load beam. Two 489 kN (110 kip) actuators were mounted vertically and spanned between the outriggers and the load beam. The outriggers were rigidly fixed to the foundation beams and anchored to the strong floor. Each actuator had swivels at both ends to accommodate in-plane movements while preventing flexural loading of the piston rods. Out-of-plane movements were restrained at the end of the beam stub.

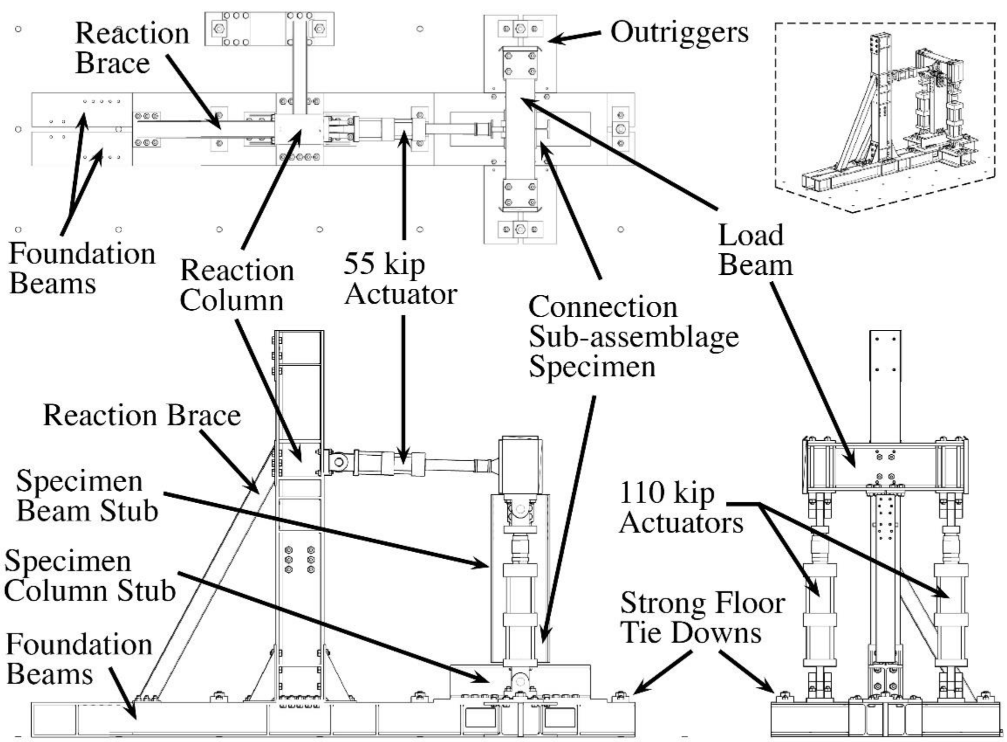

Figure 2. Connection test setup (1 kip = 4.448 kN).

Axial extension and rotation demands were applied quasi-statically to the connection sub-assemblage specimens through the load beam by the three independent actuators fixed to the reaction frame. The actuators were operated in displacement control. The displacements were computed by assuming a simple geometric relation between the extension and rotation demands at the connection and the centerline deflection of the interior column location in a simulated two-span system as shown in Fig. 3(a). The column was assumed to deflect perfectly vertically downward, and all deformations were assumed to occur at the connections about the centers of gravity of the connection bolt groups.

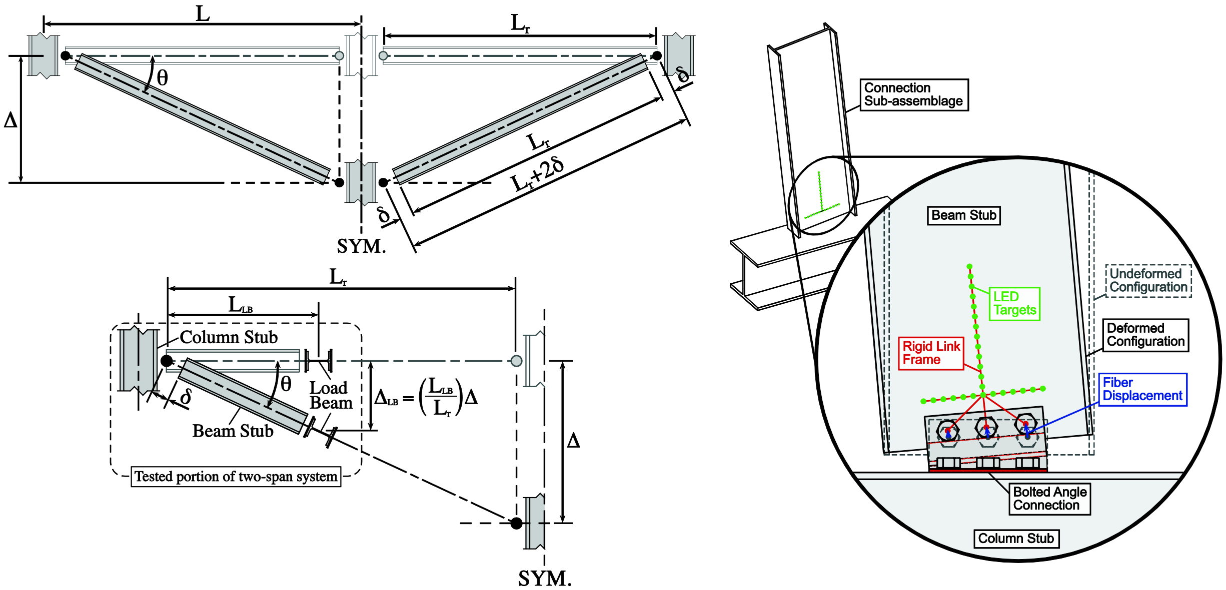

(a) (b)

Figure 3. (a) Deformed two-span system used for determining applied rotation and displacement. (b) Fiber displacements computed from light-emitting diode (LED) targets.

Considering these assumptions, the applied rotation, θ, and simultaneously applied axial extension, δ, were:

$$\theta = tan^{-1}\left(\frac{\Delta}{L_r}\right) \quad (1)$$

$$\delta = \frac{L_r}{2}\left[\sqrt{1+\left(\frac{\Delta}{L_r}\right)^2} - 1\right] \quad (2)$$

respectively, where all terms are as shown in Fig. 3. See Weigand and Berman (2014) for more details on the derivation of Eq. (1) and Eq. (2).

EXPERIMENTAL RESULTS

Experimental results are shown in Table 1 and Table 2. The estimated uncertainty in the measured data was ±1 %, based on repeated calibrations of the instruments over the course of testing. Results presented for each connection include the maximum connection rotation θ, maximum corresponding vertical displacement at the simulated damaged column, Δ, using the span lengths in Table 1 and a 9.1 m (30 ft) span for all bolted angle specimens, the maximum fiber displacement d_f, the maximum shear force at the columns face (aligned with the column), V_{max}, the maximum tension force in the connection (aligned perpendicular to the shear force), T_{max}, the maximum shear force normalized by each connection's nominal strength, V_{max}/V_{Nom}, and the failure mode. Complete discussions of the results may be found in Weigand (2014), Weigand and Berman (2015) and Weigand and Berman (2016).

To account for the combined contributions to bolt and plate deformations from the rotation and axial extension demands, the connection was discretized into individual component-width segments (fibers) each made up of a single bolt and the tributary width of beam web, and shear plate or angle. The locations of the fibers were determined prior to the application of load, with fiber-nodes centered at the light-emitting diode (LED) targets on the connection bolt-heads. One node of each fiber was assumed to be rigidly attached to the fixed specimen column stub, and the other was assumed rigidly attached to the beam web. The kinematic motions of the beam web fiber-nodes were computed by imposing a rigid-link structure onto the grid of LED targets positioned on the beam web (Fig. 3(b)). Experimental fiber displacement profiles were computed as the vectors spanning from the undeformed to the deformed locations of the fiber nodes, and decomposed into axial and shear components.

As shown in Table 1 and Table 2, different failure modes were observed depending on connection configuration and specific parameters (i.e., shear plate thickness, angle thickness, bolt diameter, etc.). Fig. 4 illustrates the progression of deformation and eventual failure for two single-plate shear specimens, one with a thinner plate (sps3b|SSLT|34|14|) that had a tearout failure and one with a thicker plate (sps3b|SSLT|34|38|) that had a bolt shear rupture failure.

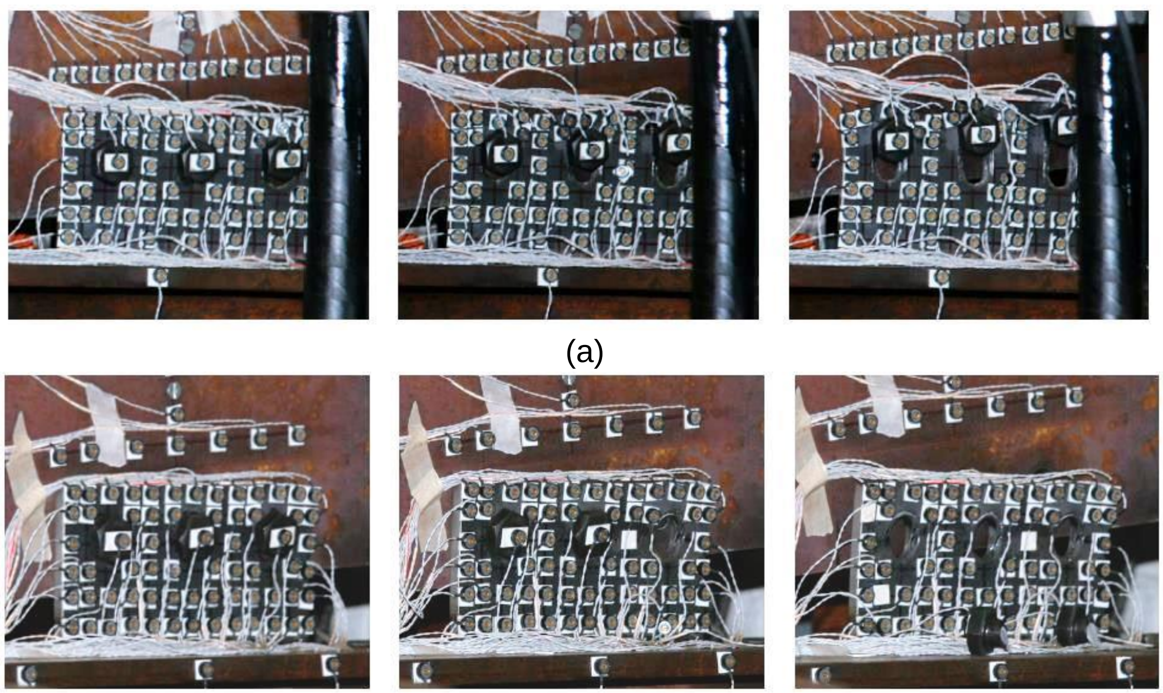

(a)

(b)

Figure 4. (a) Example of progression of plate tearout rupture in Specimen sps3b|SSLT|34|14| (b) example of bolt shear rupture in Specimen sps3b|SSLT|34|38|

The performance of connection specimens across the parameter space resulted in several key observations for gravity connections subjected to combined rotations and axial deformations. For steel single-plate shear connections:

1. The vertical shear force at the column face at connection failure is much lower than the nominal shear strength of the connection. The presence of tension in the connection greatly reduces the shear capacity. Table 1 illustrates this, as the maximum vertical shear force normalized by the nominal shear strength (V_{max}/ V_{Nom}) is typically less than 0.13.
2. Failure is generally controlled by the deformation capacity of the outer fiber. Deeper connections with more bolts have larger strength, but less deformation capacity (both rotation and tension) than shallower connections and their increase in strength is less than the increase in their nominal shear strength. This is illustrated in Fig. 5, which shows test results for three single-plate shear connections with 3 bolts, 4 bolts, and 5 bolts. The increase in vertical shear capacity (see Fig. 5(a)) is not proportional to the increase in nominal strength due to the increased number of bolts (i.e., the 4-bolt and 5-bolt connections achieved smaller percentages of their nominal strengths than the 3 bolt connection, as shown in Fig. 5(b)). Fig. 5(c) shows that the axial displacement capacity of the outer fiber of each connection was the approximately the same.
3. Connections with short slotted holes achieve larger shear forces at the column face than connections with standard holes (e.g., compare results from sps3b|STD|34|38| and sps3b|SSLT|34|38| in Table 1).
4. Binding of the beam and column flanges has a negative impact on connection performance but is unlikely to occur in typical connection configurations due to the large axial deformations at the connections (see Weigand and Berman (2014) for more details).

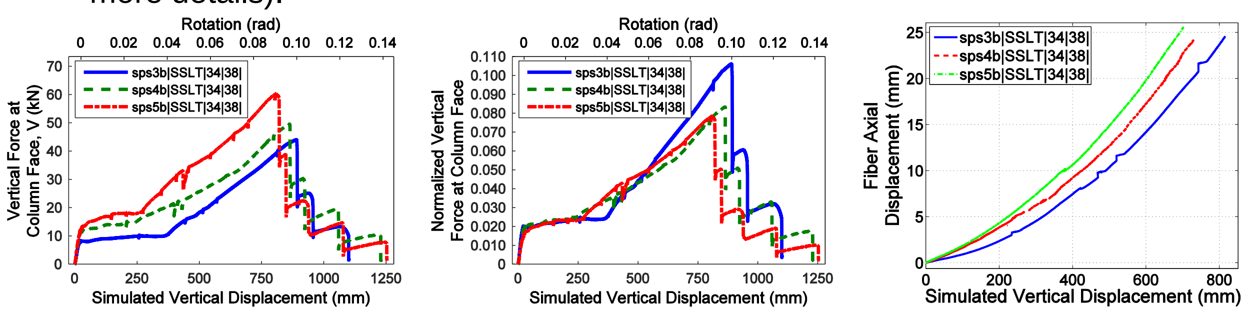

(a) (b) (c)

Figure 5. Comparison of (a) vertical force at column face normalized by connection nominal shear strength (b) horizontal force at the column face normalized by the plate tension strength, and (c) the displacement profiles in the outer fiber for 3 bolt (blue), 4 bolt (green) and 5 bolt (red) single-plate shear connections (profiles terminated at connection failure.

The key observations from the results of the tests on bolted angle specimens subjected to combined large rotations and axial deformations are:

1. For each pair of connections that differed only by angle thickness (e.g., Specimens ba3b|34|14| and ba3b|34|12|, Specimens ba5b|34|14| and ba5b|34|12|, etc.), the thicker bolted angle specimens achieve larger vertical force at the column face (Fig 6(a)).

2. Increasing the number of bolts reduces the deformation capacity of the connections and results in smaller normalized maximum vertical forces at the columns face as shown in Fig. 6(b).
3. Double angle connections with one leg welded (i.e., Specimens ba3b|34|14|BlegWeld and ba3b|34|14|ClegWeld) have reduced strength and ductility relative to bolted-bolted connections (see Table 2).
4. Double angle connections have larger deformation capacity, but lower strength than single-plate shear connections with the same nominal shear strength as shown in Fig. 7.

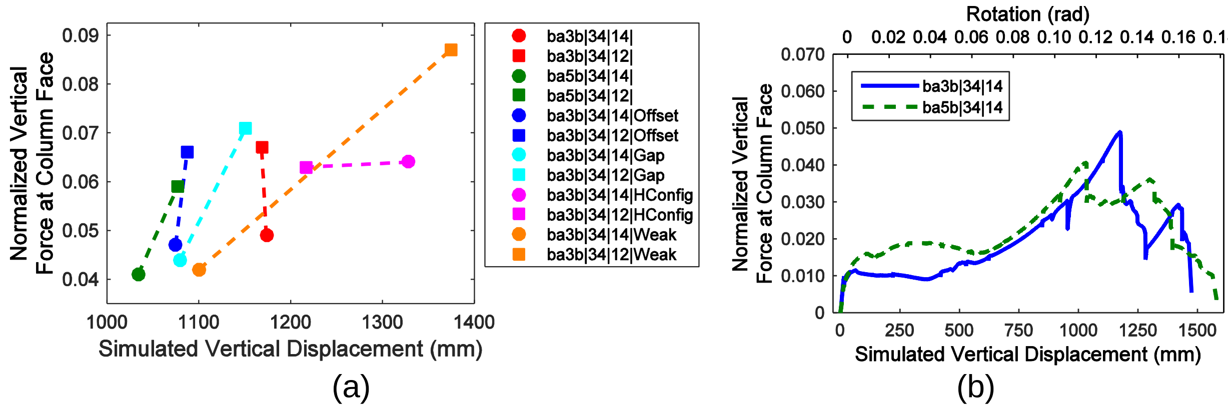

Figure 6. Comparison between (a) vertical capacities of bolted web angle connections with 6.35 mm (1/4 in.) thick and 12.7 mm (1/2 in.) thick angles normalized by connection nominal shear strength (connections of the same configuration but different angle thicknesses are connected via dashed line), and (b) vertical force at column face normalized by connection nominal shear strength for 3 bolt (blue) and 5 bolt (green) double angle connections.

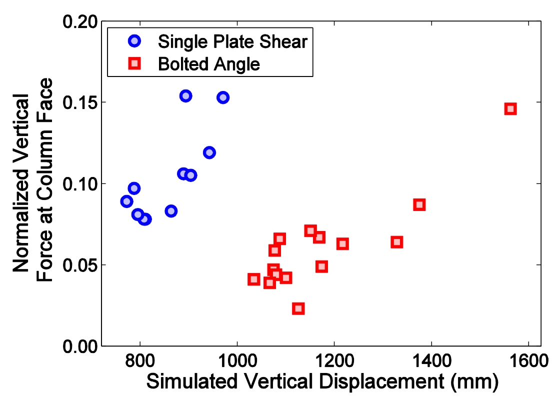

Figure 7. Maximum vertical force at column face normalized by connection nominal shear strength versus the maximum simulated vertical displacement at the removed column for all tested single-plate shear and double angle connections.

SUMMARY AND CONCLUSIONS

Tests on steel gravity framing system connections subjected to combined large rotation and tension were performed to investigate their potential contribution to structural robustness. These tests showed that such connections are adversely affected by the large deformation demands associated with a column loss scenario and often are able to resist vertical forces at the column face of less than 15 % of their nominal shear strength. The connection strength and ductility are limited by the demands on the outer fiber (i.e., the outermost bolt and tributary plates or angles) and the limiting deformations of those outer fibers were quite consistent across connections with different depths.

ACKNOWLEDGEMENTS

This research was supported by the American Institute of Steel Construction (AISC) and the National Science Foundation under Grant No. CMMI-1000926. The steel wide flange sections used in the experiments were donated by AISC. Any opinions, findings, conclusions, and recommendations are those of the authors, and do not necessarily reflect the views of the sponsors.

REFERENCES

Astaneh-Asl, A., Jones, B., Zhao, Y., and Hwa, R. (2001). “Progressive collapse resistance of steel building floors." Report No. UCB/CEE-Steel-2001/03, University of California at Berkeley, Dept. of Civil and Environmental Engineering.

Astaneh-Asl, A., Madsen, E., Noble, C., Jung, R., McCallen, D., Hoehler, M. S., Li, W., and Hwa, R. (2001). “Use of catenary cables to prevent progressive collapse of buildings." Report No. UCB/CEE-Steel-2001/02, University of California at Berkeley, Dept. of Civil and Environmental Engineering.

Foley, C. M., Martin, K., and Schneeman, C. (2006). “Robustness in structural steel framing systems." Report No. MU-CEEN-SE-06-01, Marquette University.

Khandelwal, K., Kunnath, S., El-Tawil, S., and Lew, H. (2008). “Macromodel-based simulation of progressive collapse: Steel frame structures." Journal of Structural Engineering, 134(7), 1070-1078.

Main, J. A. and Sadek, F. (2013). \Modeling and analysis of single-plate shear connections under column loss." Manuscript Accepted to Journal of Structural Engineering.

Oosterhof, S. A. and Driver, R. G. (2012). “Performance of Steel Shear Connections under Combined Moment, Shear, and Tension." ASCE/SEI Structures Congress, Chicago, IL. 146-157.

Sadek, F., El-Tawil, S., and Lew, H. S. (2008). “Robustness of composite floor systems with shear connections: Modeling, simulation, and evaluation." Journal of Structural Engineering, 134(11), 1717-1725.

Thompson, S. L. (2009). “Axial, shear and moment interaction of single plate “shear tab" connections," PhD thesis, Milwaukee School of Engineering.

Weigand, J. M. (2014). “The Integrity of Steel Gravity Framing System Connections Subjected to Column Removal Loading." Ph.D. Dissertation in Civil Engineering, University of Washington, Seattle, WA (June).

Weigand, J. M. and Berman, J.W. (2014). “Integrity of Steel Single Plate Shear Connections Subjected to Simulated Column Removal." Journal of Structural Engineering, 140(5), 04013114.

Weigand, J. M. and Berman, J.W. (2016). “Integrity of Bolted Angle Connections Subjected to Simulated Column Removal." Journal of Structural Engineering, 142(3), 04015165.

Weigand, J. M., Meissner, J. E., Francisco, T., Berman, J. W., Fahnestock, L. A., and Liu, J. (2012). “Testing the Integrity of Steel Gravity Frames subjected to Large Vertical Deflections: Components." ASCE/SEI Structures Congress, Chicago, IL (March).